Silicon carbide-induced piezoelectric β-phase in poly(vinylidene fluoride) and its properties

Jay Sheth and Devendra Kumar
Department of Ceramic Engineering, Institute of Technology, Banaras Hindu University, Varanasi-221005, India
Vimal K. Tiwari and Pralay Maiti[a)]
School of Materials Science and Technology, Institute of Technology, Banaras Hindu University, Varanasi-221005, India

(Received 8 December 2011; accepted 14 March 2012)

The piezoelectric β-phase of poly(vinylidene fluoride) (*PVDF*) has been synthesized through solution route in presence of varying percentage of silicon carbide (*SiC*). Various measurements were conducted to analyze the effect of *SiC* addition on structural, mechanical, and dielectric properties, as also the properties affecting hydrophilicity and morphology of *PVDF*. The x-ray diffraction, Fourier transform infrared spectroscopic and differential scanning calorimetry analyses confirm the presence of β-phase of *PVDF* on addition of *SiC*. The Young's modulus of the composites increases as compared with pristine *PVDF*. The hydrophilic nature of the composites improves with increasing *SiC* content. Dielectric constant increases in composites, especially at lower frequency range and the relaxation pattern in the crystalline phase changes significantly causing reduction of relaxation frequency with increasing *SiC* concentration.

I. INTRODUCTION

Poly(vinylidene fluoride) (*PVDF*) is a semi crystalline polymer that has drawn both scientific and technological attentions because of the useful pyroelectric[1] and piezoelectric[2] properties. It is also one of the rare polymers that exhibit diverse crystalline forms, having five different phases known as α, β, γ, δ and ε.[3–5] The polar phases e.g., β and γ are technologically most interesting because of its better pyroelectric and piezoelectric properties. Other notable properties of *PVDF* are its typical fluoropolymer characteristics like hydrophilicity and high mechanical strength. Because of these properties *PVDF* has been considered as a good candidate for the following sensing applications: pressure,[6] temperature,[7] gas,[8] and electromagnetic wave sensors. It is also used in nonlinear optics[9] and microwave transducers.[10] *PVDF* is water-resistive material; therefore, it is suitable for outdoor and indoor paint.[11] Moreover, it has important medical applications[12] because of its nonrejectability in human tissues.

Various studies on *PVDF* have been previously conducted to analyze the effect of addition of different fillers on physical properties of the composites. Blending with poly(methyl methacrylate) (PMMA) was described as an original way to force *PVDF* to crystallize into the piezoelectric phase, which is thermodynamically unstable in pure material.[13] Abdelaziz et al. investigated the physical properties of *PVDF* films filled with $CuCl_2$[14] and $MnCl_2$.[15] These investigations revealed that these fillers modified the structural, electrical, and/or magnetic properties of the matrix *PVDF*. However, a nonlinear (even nonmonotonic) filling level (FL)-dependence on the contents of the active structural forms was found. Piezoelectric β-form can usually be crystallized by applying suitable conditions like poling at high voltage,[16] recrystallization of carbon-coated highly oriented ultra thin film[17] and molecular epitaxy on the surface of potassium bromide.[18] Addition of nanofillers like nanoclay[19] and carbon nanotube (CNT)[20] shows the growth of β-form in *PVDF*. Shah et al. added nanoclay to *PVDF* to form nanocomposites and reported a remarkable enhancement in the toughness.[21] The addition of calcium sulfate whiskers to *PA66/PVDF* blends improves the tensile and flexural performances.[22] Addition of ceramic material to a high strength polymer is an interesting and inexpensive method to modify various properties of a polymer. Silicon carbide (*SiC*) ceramic offers excellent strength, chemical resistance at high temperature, semi-conductivity, high thermal stability and thermal conductivity for uses as high-temperature structural materials as well as in electric devices that function at elevated temperatures.[23,24]

In this work, we study the effect of addition of silicon carbide (*SiC*) to various properties of *PVDF*. The α to β phase transition has been characterized by x-ray diffraction (*XRD*) and Fourier transform infrared (*FTIR*) spectroscopic analyses. The thermal analysis is performed by using differential scanning calorimetry (*DSC*) to show the structural change. Optical micrographs and scanning

[a)]Address all correspondence to this author.
e-mail: pralay_maiti@yahoo.com
DOI: 10.1557/jmr.2012.117

 © Materials Research Society 2012

https://doi.org/10.1557/jmr.2012.117 Published online by Cambridge University Press

electron micrographs show deformation of spherulite structure of *PVDF* due to incorporation of *SiC* particle. We also report the mechanical properties, contact angle measurement, dielectric relaxation and resistivity after the incorporation of *SiC* for evaluating cause of alteration in presence of *SiC*.

II. EXPERIMENT

A. Materials

A commercial *PVDF*, (SOLEF 6008; Ausimont, Milano, Italy), was used in this work and was prepared into films of 0.2 mm thickness by compression molding. The laboratory-grade *SiC* was purchased from Carborundum Universal Ltd. (Chennai, India) in powder form.

Composite preparation

The composite was prepared by solution casting method. The *PVDF* was dissolved in dimethyl formamide (*DMF*) solvent at 60 °C. Measured quantity of SiC powder was added to the solution and was stirred to ensure homogeneous mixing. After good dispersion at suitable viscosity, the composite film was prepared by casting onto a glass Petri dish and left to evaporate the solvent slowly by heating it and thereafter, it was kept in vacuum oven at 60 °C for 48 h for complete removal of solvent from composites. The *SiC* concentration was varied in composite film. Four films of composition *PVDFCx* were prepared where x is the weight percent of *SiC* added and $x = 0, 2, 5, 10$.

B. Characterization

1. *XRD* Analysis

XRD experiments were performed using a Bruker AXS D8 Advance wide-angle x-ray diffractometer (Madison, WI) with Cu K_α radiation and a graphite monochromator (wavelength, $\lambda = 0.154$ nm). The generator was operated at 40 kV and 40 mA. Thin films of pure *PVDF*, its composites and a pallet of *SiC* were placed on a quartz sample holder at room temperature and were scanned at diffraction angle 2θ from 1° to 40° at a scan rate of 1°/min to explore the nanostructure and crystalline structure of pure *PVDF* and its composites.

2. FTIR analysis

FTIR analysis of pure *PVDF* and its composites was done from 1000 to 500 cm^{-1} using very thin films of the composites and pure *PVDF*.

3. DSC analysis

The melting temperature, crystallization temperature and heat of fusion of pure *PVDF* and its composites were measured in a Mettler 832 DSC instrument (Greifense, Switzerland). The samples were heated at a scan rate of 10 °C/min. The peak temperature and enthalpy of fusion were measured from the endotherm using standard software. After the first melting, the samples were cooled down at a constant rate of 10 °C/min to find the crystallization temperature and heat of crystallization in a similar fashion. Further, a second heating was taken to ensure the amount of crystallinity and melting temperature after removing all the thermal history in the first run. The DSC was calibrated with indium and zinc before use.

4. Polarized optical microscope image

Spherulitic growth was observed using an Olympus optical microscope (Tokyo, Japan). The photographs were captured with the help of a camera attached to the microscope at a magnification of 500×.

5. Mechanical strength

Tensile tests were performed on the microinjected dog bone shaped samples at room temperature using a universal testing machine (Instron, Norwood, MA) at a strain rate of 5 mm/min. Two samples were tested for each specimen.

6. Contact angle

Contact angle measurement of pure *PVDF* and its composites was carried out by using Kruss F-100 tensiometer (Hamburg, Germany). The strip was immersed in water at room temperature and the contact angle was measured in advance mode.

7. Two-probe conductivity

The DC electrical resistivity was measured of pure *PVDF* and its composites at room temperature. The films of the specimens were coated with a homogeneous layer of silver paste. This paste was allowed to dry before carrying out the measurements.

8. Dielectric measurements

Dielectric measurements were performed on disc-shaped films of 11.1 mm diameter. The samples were silver-coated on opposite faces and the measurements were carried out between frequencies 10^{-3} to 10^7 Hz in a high-resolution dielectric analyzer (Novocontrol Alpha A high performance frequency analyzer, Hundsangen, Germany). The accuracy of dielectric analyzer is 0.2%.

III. RESULTS AND DISCUSSION

A. Structural change

The x-ray diffraction patterns of pure *PVDF*, pure *SiC* and their composites with 5 and 10 wt% of SiC in *PVDF* matrix have been shown in Fig. 1. Pure *PVDF* crystallizes

https://doi.org/10.1557/jmr.2012.117 Published online by Cambridge University Press

in stable α phase with characteristic peaks at 17.6°, 18.3° and 19.9°, corresponding to (110), (020) and (111) crystal planes, respectively. In case of pure *SiC*, the diffraction peak at 2θ = 30.9°, corresponding to the plane (111). The diffraction peak for *PVDFC5* at 2θ = 20.1° is due to formation of β phase corresponding to the plane (200/110) together with predominant α phase diffraction peaks. A shifting toward higher angle is also observed with increase in SiC content. The diffraction peak for (200/110) plane of *PVDFC10* is observed at 2θ = 20.2° showing more β content. Thus, it is observed that the β content increases with increase in *SiC* content affecting the nature of crystallization in presence of *SiC* particles.[25,26] The crystalline peak position, crystallite size and peak assignments of all the major peaks are listed in Tables IA and IB. The crystallite size of *PVDF*, as measured using Scherrer equation, decreases with increasing *SiC* content due to favorable interaction between polymer and *SiC* particle. The crystallite size of *SiC* increases with increase of the percentage of *SiC* in composite due to agglomeration. Figure 2 shows the FTIR spectrum of *PVDF* and its composites in the range of 500–1000 cm^{-1}. The α crystalline peaks of pure *PVDF* are clearly observed at 763 and 796 cm^{-1} but the peak intensity gradually diminishes with increasing *SiC* content. Simultaneously, strong β-peaks at 840 and 510 cm^{-1} are observed in composites, corresponding to CH_2 rocking and CF_2 asymmetric stretching indicating a change in the crystal structure of the polymer in presence of SiC. The absorption band at 763 cm^{-1} is related to in-plane bending vibration. The FTIR analyses, therefore, support the formation of piezoelectric β-phase in presence of *SiC*. It is worth mentioning here that the peaks from x-ray and FTIR assigned for β phase are quite broad, indicating the presence of some mixed α-phase as well. Therefore, it can be concluded that the polymer chains, away from the surface of *SiC* particles crystallize in α-phase and those chains which are in close proximity of *SiC* crystallizes in β-phase. The assignment of the peaks is in agreement to the result reported in the literature.[26,27]

B. Thermal behavior

DSC thermograms of *PVDF* and *PVDFC5* are presented in Figs. 3(a) and 3(b) for the heating and cooling processes. *PVDF* shows double melting peaks primarily due to melt recrystallization indicative of α-phase. But, incorporation of *SiC* in polymer matrix show much higher melting temperature than that of pure *PVDF*. The melting points are 169.7° and 175.9 °C for pure *PVDF* and *PVDFC5*, respectively. Higher melting peak for composite also suggests the formation of β-phase.[26] Heat of fusion (ΔH) of pure *PVDF* and *PVDFC5* are 61 and 27 J.gm, respectively. Reduction of ΔH in composites is due to induced β-phase of *PVDF* in presence of SiC. Figure 3(b) compares the cooling isotherms of *PVDF* and *PVDFC5*

TABLE IA. The values of 2θ and respective d spacing for PVDF peaks as observed in the x-ray diffraction scans.

SiC wt%	2θ	FWHM (in radians)	τ = kλ/βcosθ (angstrom)	Assignment
0	19.947	0.0130	108	(111)α
5	20.054	0.0151	93	...
10	20.194	0.0189	74.5	(200/110)β

TABLE IB. The values of 2θ and respective d spacing for SiC peaks as observed in the x-ray diffraction scans.

SiC wt%	2θ	FWHM (in radians)	τ = kλ/βcosθ (angstrom)	Assignment
5	31.03	0.0416	34.6	(111)
10	31.08	0.0159	90.5	(111)
100	30.99	0.0033	435.8	(111)

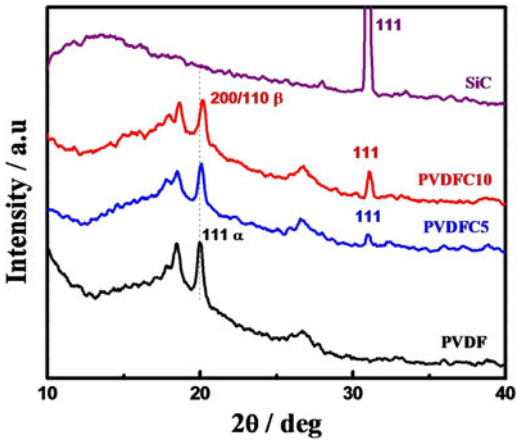


FIG. 1. *XRD* patterns showing development of β phase in PVDF- SiC composites.

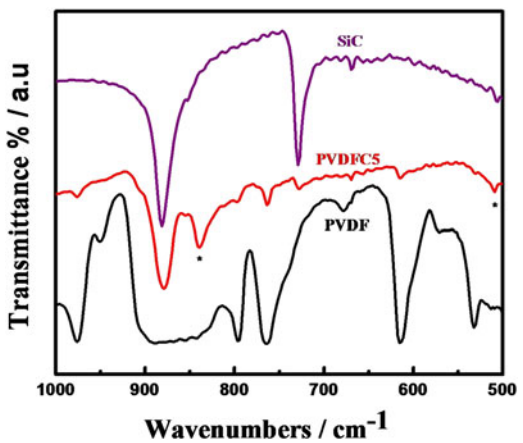


FIG. 2. *FTIR* curves showing appearance of β peak marked with (*) in PVDFC5 composite.

https://doi.org/10.1557/jmr.2012.117 Published online by Cambridge University Press

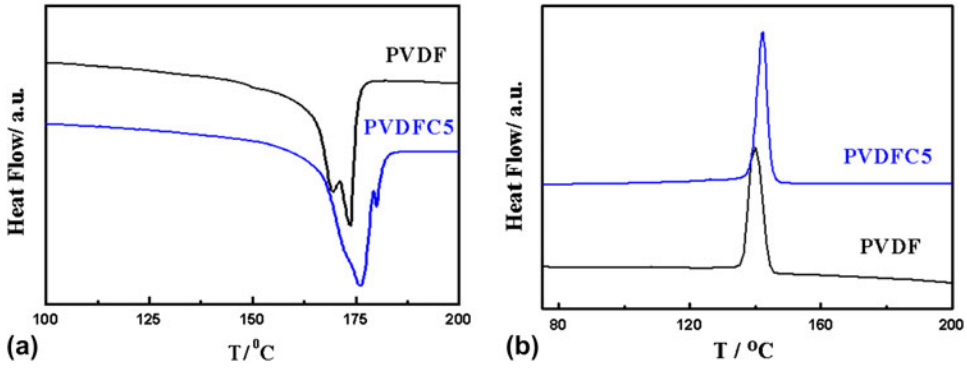


FIG. 3. *DSC* thermograms of pure *PVDF* and *PVDFC5*: (a) melting endotherm, and (b) cooling curves at a heating/cooling rate of 10 °C/min.

showing higher crystallization temperature for composite (142 °C) than that of pure *PVDF* (140 °C). Hence, *SiC* particles act as nucleating agents and, thereby, the polymer chains nucleate easily on the heterogeneous surface of *SiC* particle.

C. Surface morphology and modification

Figure 4 shows the scanning electron micrographs (SEM) of pure *SiC*, *PVDF* and *PVDFC5*. *SiC* particles are clearly visible with a wide range of flake from nanometer to micrometer size. Pure *PVDF* exhibits spherulite structure indicating α-phase in melt cast sample. On the contrary, tiny particles of *SiC* are uniformly distributed in the composite and spherulitic nature of these *PVDF* particles is also evident. We can conclude that even though there is signature of β-phase in the composite as evident from XRD, FTIR and DSC studies, significant amount of α-phase is also present in the composite. It is believed that *PVDF* crystallizes on the surface of the *SiC* particles in β−crystalline form and the polymer chains away from *SiC* particle crystallize in usual α-form. As the size of SiC particle is not small enough the overall surface area is quite small limiting the amount of β-phase in composite. In case of nanoparticles like layered silicate, the surface area is significantly high causing formation of greater quantity of β-phase[21] and there is a complete loss of birefringence in optical images as well. The appearance of spherulite with less contrast in this composite clearly indicates the presence of α-phase in addition to some β-phase primarily on top of the *SiC* flakes. The optical images also show the compact spherulite of pure *PVDF* while it becomes coarse in composite (Fig. 5). *SiC* particles create a barrier in the crystal growth front causing coarse spherulite in the composite as compared with compact and ordered spherulite in pure *PVDF*. It is also observed that the spherulites become coarser and smaller in size with increasing amount of *SiC* in the composite. Figure 6 compares the contact angle of *PVDF* in presence of *SiC* filler to investigate the hydrophilic nature of the surface.

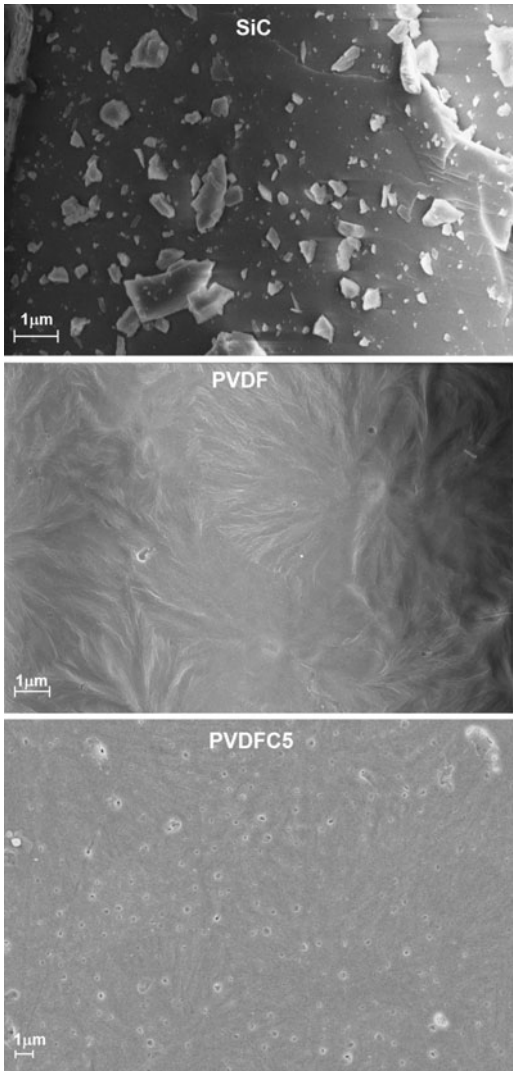


FIG. 4. SEM images of *SiC*, *PVDF* and *PVDFC5*.

Pure *SiC* is hydrophilic and thus it is expected that the water absorption of *PVDF* increases on addition of *SiC* to *PVDF*. It is clear that the contact angle of the film decreases (~4°)

https://doi.org/10.1557/jmr.2012.117 Published online by Cambridge University Press

with increase in *SiC* concentration (Fig. 6). Thus, the composite films become hydrophilic on increasing the concentration of *SiC* in the composite.

D. Mechanical property

The tests for mechanical properties under uniaxial elongation have been performed using universal testing machine. Figure 7 shows the stress-strain curves of pristine *PVDF* and a representative *PVDFC5* composite. The Young's modulus, as calculated from the slope of the linear region, of composite (*PVDFC5*) increases to 838 MPa from 745 MPa of that of pure *PVDF* while the toughness, as measured from the area under the stress-strain curve of the composite decreases to 1504 J/m^3 from 1654 J/m^3 of that of pure *PVDF*. It is obvious that the stiffness increases in composite while the toughness decreases a bit in presence of *SiC* particle, which is a typical case of filled system.[19] On the other hand, the tensile strength increases but the elongation at break decreases in composite as compared with pure PVDF.

E. Electric and dielectric properties

PVDF is an insulator and pure *SiC* usually acts as a semiconductor. The result of the resistivity measurement showed systematic decrease from 10^{14} Ω-cm of pure *PVDF* to 10^{12} Ω-cm in *PVDFC10* in presence of 10 wt% *SiC* (Fig. 8). The decrement in resistivity in composite is gradual and two orders lower in magnitude than that of pure PVDF observed at room temperature. Figure 9 shows the typical dielectric permittivity (ε′) of *PVDF* and its composites with varying frequency for different *SiC* concentration at room

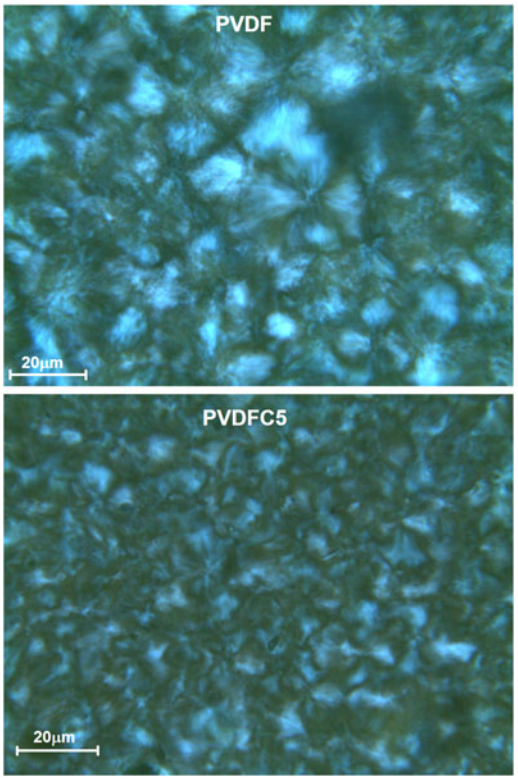


FIG. 5. Polarizing Optical images of *PVDF* and *PVDFC5*.

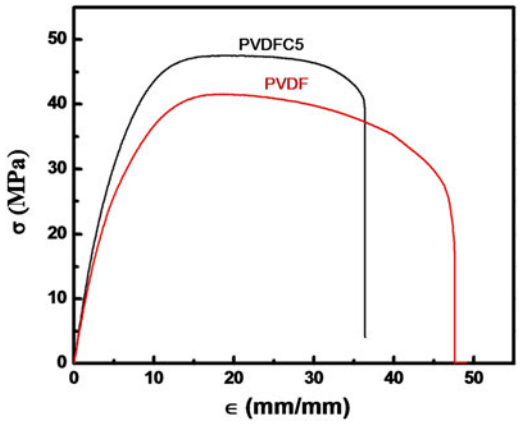


FIG. 7. Stress-strain curves for pure *PVDF* and PVDFC5 composite.

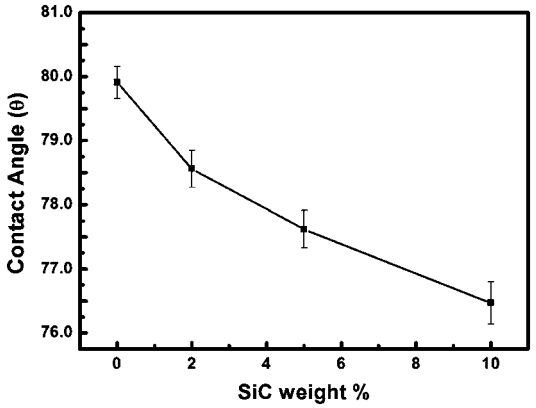


FIG. 6. Variation in contact angle with increasing *SiC* weight percentage.

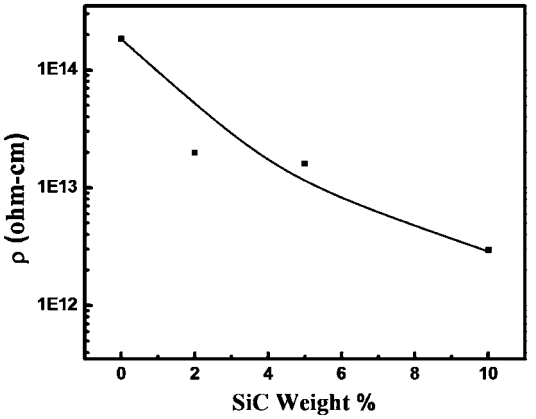


FIG. 8. Effect of increasing *SiC* concentration on resistivity of *PVDF-SiC* composites.

https://doi.org/10.1557/jmr.2012.117 Published online by Cambridge University Press

temperature. The dielectric constant increases with increase in *SiC* content. Maximum increment is observed in lower frequency range and the values are 22, 42, 57 and 150 for pure *PVDF*, *PVDFC2*, *PVDFC5* and *PVDFC10*, respectively, at 10^{-3} Hz frequency. Thus, the frequency dependence dielectric study indicates that the dielectric constant increases with the addition of *SiC* in polymer matrix especially in the low frequency region. The tan δ curves at room temperature show one relaxation peak at 7 Hz for pure *PVDF* attributed to the relaxation of molecules associated in the crystalline region (Fig. 10). The peak position has been shifted to 3 Hz (toward lower frequency side) for *PVDFC2* and interestingly, the peak has been further shifted to much lower frequency to 0.3 Hz for *PVDFC10* presumably due to change in conformation with internal rotation that occur in crystalline β phase in presence of *SiC* filler that commensurate in *XRD* and *FTIR* studies.[28] There is a tendency for a probable peak at $\sim 10^7$ Hz but that is beyond the capacity of our instrument and the peak is related to the cooperative motion of the main chain, so called glass transition temperature.[29] $BaTiO_3$ and other high dielectric constant materials increase the overall dielectric constant when they are dispersed in polymer matrix but the crystalline relaxation peak does not shift as there is no change of crystalline structure in presence of filler.[30] In this case, *SiC* nucleates β-phase in *PVDF*, thereby, the relaxation pattern in the crystalline phase changes significantly causing reduction of relaxation frequency with increasing *SiC* concentration. SiC is a good semiconductor and high dielectric constant can be explained using percolation theory in PVDFC5. In PVDF, there are three relaxations in permittivity loss curve at different frequency regions.[29,30] The α_c relaxation associated with molecular motions in crystalline region of PVDF at about 0.3–7 Hz and has been discussed here in Fig. 10. The second relaxation α_a comes around at 10^7 Hz related to the glass transition relaxation. The third relaxation attributed to Maxwell-Wagner-Sillars (MWS) polarization comes due to interfacial polarization at very low frequency ($<10^{-4}$ Hz) in pure PVDF.

The temperature-dependent dielectric properties have been analyzed for both pure PVDF and PVDFC5 to compare dielectric constant and relaxations due to permittivity loss of pure PVDF in nonpolar phase and PVDFC5 composite with β-polar phase. The dielectric permittivity of the PVDF and PVDFC5 at different temperatures are given in Fig. 11(a). Dielectric permittivity has increased with increasing temperature both for pure PVDF and PVDFC5. PVDF have dielectric constants of 13, 28, 37 and 61 at temperature 30, 60, 80 and 100 °C, respectively, at 1 Hz frequency. PVDFC5 have dielectric permittivity of 14, 28, 52 and 62 at same temperatures mentioned above showing bit higher values for composite. Figure 11(b) exhibits tan δ curves of PVDF and PVDFC5 measured at different temperatures. It shows the shifting of crystalline relaxation peak position to higher frequency

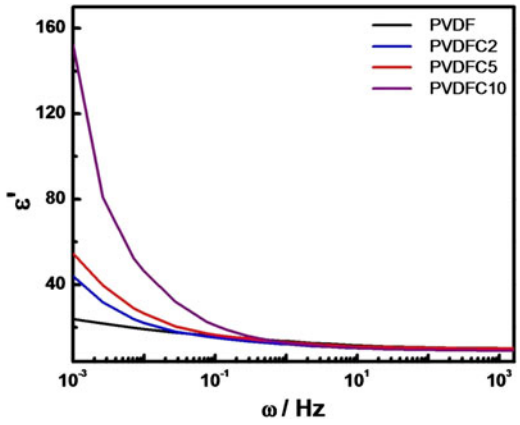


FIG. 9. Dielectric real part (ε′) as a function of frequency (ω) for the prepared composite films with different *SiC* concentration.

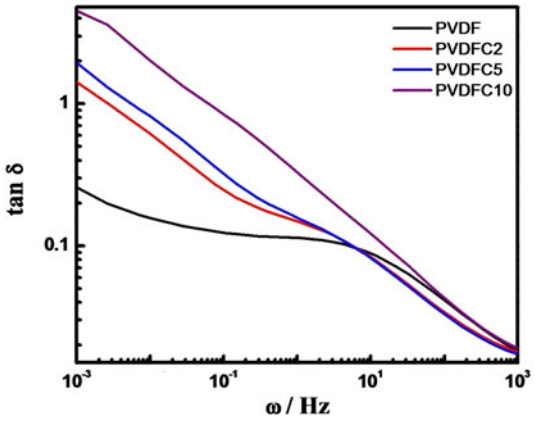


FIG. 10. Dielectric loss as a function of frequency for the prepared composite films with different SiC concentration.

range with increase in temperature both for PVDF and PVDFC5. The temperature-dependent dielectric relaxation and its interactions in presence of semiconducting SiC is explained by Havriliak-Negami (H-N) function[30,31]:

$$\varepsilon^* = -i\frac{\sigma_{dc}}{\varepsilon_0 \omega^s} + \varepsilon_\infty + \sum_j \frac{(\Delta\varepsilon)_j}{[1+(iw\tau_j)^\alpha]^\beta} \quad ,$$

where, σ_{dc} is direct current conductivity, ω is the angular frequency, s is an exponent ($0 < s \leq 1$), τ_j is the relaxation time of the j^{th} process, ε_0 is the vacuum permittivity, Δε is the dielectric strength of the j^{th} process and α and β are the shape parameters of the H-N function that define the breadth and the symmetry of the spectrum. Width parameter α specifies the slope of the low frequency side of the relaxation behavior of ε″ curve and β is the asymmetry parameter and it is calculated using the slope of the relaxation behavior at the high frequency side of the same pattern as—αβ. The analyses through H-N function using WinFit software program of PVDF and PVDFC5 have been given in Table II using deconvoluted H-N fits (Fig. 12). In

https://doi.org/10.1557/jmr.2012.117 Published online by Cambridge University Press

PVDF, β parameter has the value of 1 for the temperature range measured showing symmetry of spectrum, but PVDFC5 has different values (~0.54–0.70) due to presence of mutliphase after interaction with SiC particles. Relaxation time (τ) calculated from H-N fit using WinFit software decreases with increase in temperature both for PVDF and PVDFC5, whereas the relaxation time for PVDFC5 shows lower value as compared with pure PVDF. However, we demonstrate the nucleation of piezoelectric β-phase in *PVDF* in presence of *SiC* filler. Subsequent improvement in mechanical, thermal, hydrophilicity, electric and dielectric properties have been revealed in association with the induced β-phase by the filler. The relaxation phenomenon in presence of filler has been explained.

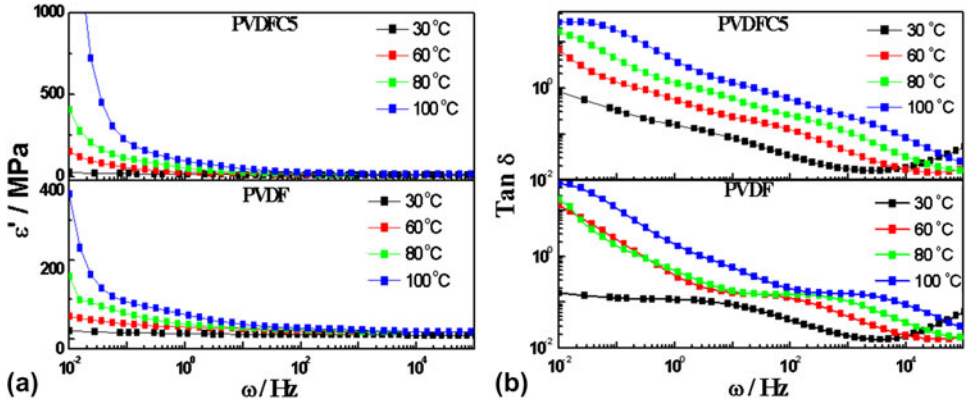


FIG. 11. Dielectric loss as a function of frequency for the pure PVDF and PVDFC5 at various temperatures.

TABLE II. Fitting parameters for α_c relaxation as a function of temperature obtained from H-N fits.

Temp. (°C)	PVDF α	PVDFC5 α	PVDF β	PVDFC5 β	PVDF τ (Sec.)	PVDFC5 τ (Sec.)
30	0.55	0.67	1	0.54	2.56E-1	5.36E-1
60	0.56	0.50	1	0.59	7.38E-3	1.66E-1
80	0.49	0.63	1	0.79	5.08E-3	9.2E-2
100	0.56	0.81	1	0.70	7.54E-4	1.56E-2

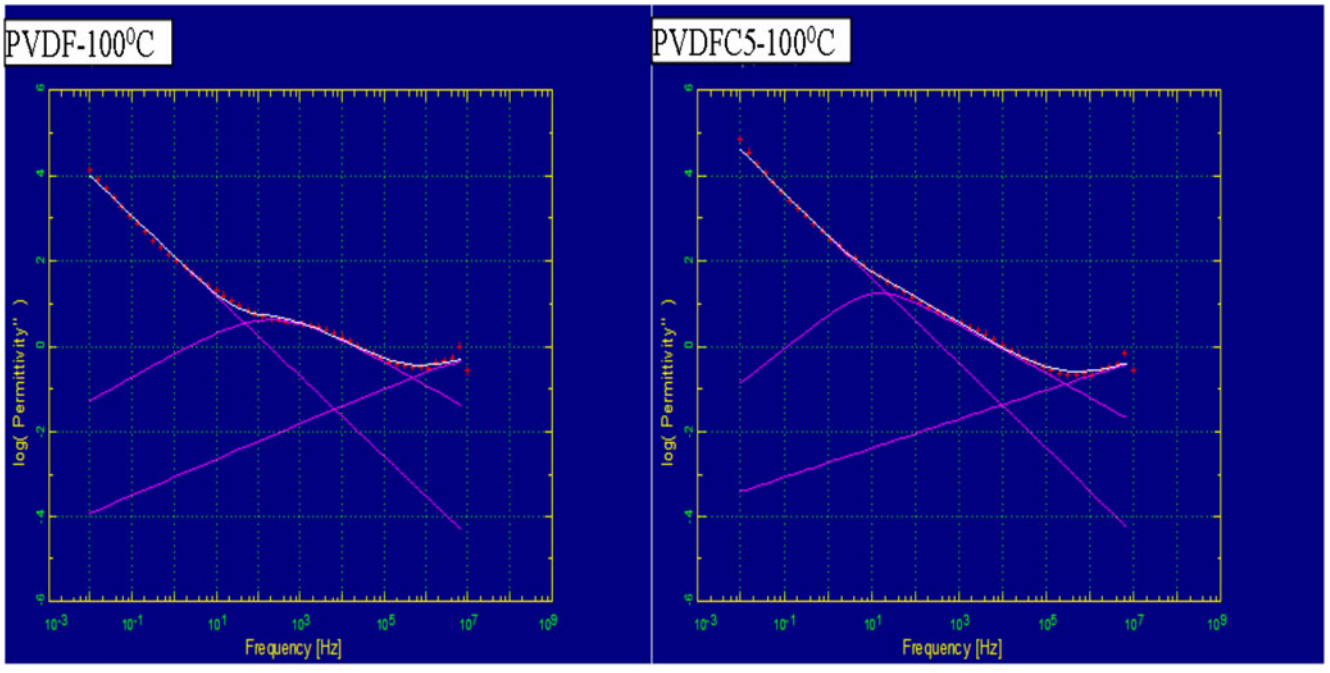


FIG. 12. Dielectric loss in the frequency domain and spectrum was deconvoluted from H-N fits.

https://doi.org/10.1557/jmr.2012.117 Published online by Cambridge University Press

IV. CONCLUSION

The composite of *PVDF* has been synthesized in presence of varying *SiC* content through solution route. The piezoelectric β-phase has been nucleated in presence of *SiC* particle. The existence of β-phase has been confirmed by using *XRD*, *FTIR* and *DSC* studies. The hydrophilicity of the composites increases with *SiC* content as the contact angle decreases with increasing *SiC* content in the composites. The tensile modulus improves in composite as compared with pristine *PVDF* while there is slight reduction in toughness. Change in structural conformation has been reported in composite (β-phase) in presence of *SiC* filler as evident from the shift of peak position to lower frequency in composite vis-à-vis pure *PVDF*. The relaxation behavior occurs at higher frequency with increasing temperature and the fitting of the curves provide the insight of the shape parameters of the relaxation phenomena indicating interaction between matrix PVDF and SiC particle causing nucleation of piezoelectric phase.

REFERENCES

1. Y. Takahashi and H. Tadakoro: Crystal structure of form III of poly (vinylidene fluoride). *Macromolecules* **13**, 1317 (1980).
2. Y. Takahashi, Y. Matsubara, and H. Tadakoro: Crystal structure of form II of poly(vinylidene fluoride). *Macromolecules* **16**, 1588 (1983).
3. Q. Gao and J.I. Scheinbeim: Dipolar intermolecular interactions, structural development, and electromechanical properties in ferroelectric polymer blends of nylon-11 and poly(vinylidene fluoride). *Macromolecules* **33**, 7564 (2000).
4. M. Benz and W.B. Euler: Determination of the crystalline phases of poly(vinylidene fluoride) under different preparation conditions using differential scanning calorimetry and infrared spectroscopy. *J. Appl. Polym. Sci.* **89**, 1093 (2003).
5. P. Maiti, J. Chatterjee, D. Rana, and A.K. Nandi: Melting and crystallization behaviour of poly(vinylidene fluoride) samples in its blends with some polyacrylates, poly(vinyl esters) and poly(aryl ether ether ketone). *Polymer* **34**, 4273 (1993).
6. G.E. Johnson, L.L. Blyler, G.R. Crane, and C. Gieniewski: Thermal piezoelectric stability of poled uniaxially oriented and biaxially oriented poly(vinylidene fluoride). *Ferroelectrics* **32**, 43 (1981).
7. E. Jassa and K. Arshak: The use of PE/PVDF pressure and temperature sensors in smart wireless sensor network system developed for environmental monitoring. *Sens. Lett.* **6**, 1 (2008).
8. Y. Takse and A. Odajima: Ferroelectric polarization switching in polyvinylidene fluoride. *Jpn. J. Appl. Phys., Part 2* **21**, L707 (1982).
9. T. Naoto, U. Yashiaki, and K. Tsuyoshi: Thermal stability of internal electric field and polarization distribution in blend of polyvinylidene fluoride and polymethylmethacrylate. *J. Appl. Phys.* **74**, 3366 (1993).
10. A. Tawansi, H.I. Abdelkader, W. Balachandran, and E.M. Abdelrazek: FeCl3 doped polyvinylidene fluoride part II pauli susceptibility and microwave response. *J. Mater. Sci.* **29**, 4001 (1994).
11. S.T. Hughes and A.R. Piery: The simultaneous measurement of pyroelectric and relaxation currents in poly(vinylidene fluoride). *J. Phys. E: Sci. Instrum.* **19**, 976 (1986).
12. R.F. Valentini, T.G. Vargo, J.A. Gardella, and P. Aebischer: Patterned neuronal attachment and outgrowth on surface-modified, electrically charged fluoropolymer substrates. *J. Biomater. Sci., Polym. Ed.* **5**, 13 (1993).
13. C. Leonard, J.L. Halary, and L. Monnerie: Crystallization of poly (vinylidene fluoride)-poly(methyl methacrylate) blends: Analysis of the molecular parameters controlling the nature of poly(vinylidene fluoride) crystalline phase. *Macromolecules* **21**, 2988 (1988).
14. A. Tawansi, M.I. Ayad, and E.M. Abdelrazek: Effect of valence electron spin polarization on the physical properties of $CuCl_2$-filled poly(vinylidene fluoride) as a microwave modulator. *J. Appl. Polym. Sci.* **72**, 771 (1999).
15. A. Tawansi, A.H. Oraby, E.M. Abdelrazek, M.I. Ayad, and M. Abdelaziz: Effect of local structure of $MnCl_2$-filled PVDF films on their optical, electrical, electron spin resonance, and magnetic properties. *J. Appl. Polym. Sci.* **70**, 1437 (1998).
16. J. Scheinbeim, C. Nakafuku, B.A. Newman, and K.D. Pae: High pressure crystallization of poly(vinylidene fluoride). *J. Appl. Phys.* **50**, 4399 (1979).
17. J. Wang, H. Li, J. Liu, Y. Duan, S. Jiang, and S. Yan: On the $\alpha \rightarrow \beta$ transition of carbon-coated highly oriented PVDF ultrathin film induced by melt recrystallization. *J. Am. Chem. Soc.* **125**, 1496 (2003).
18. A.J. Lovinger: Crystallization of the beta-phase of poly(vinylidene fluoride) from the melt. *Polymer* **22**, 412 (1981).
19. L. Priya and J.P. Jog: Poly(vinylidene fluoride)/clay nanocomposites prepared by melt intercalation: crystallization dynamic mechanical behavior studies. *J. Polym. Sci., Part B: Polym. Phys.* **40**, 1682 (2002).
20. S. Yu, W. Zheng, W. Yu, Y. Zhang, Q. Jiang, and Z. Zhao: Formation mechanism of β-phase in PVDF/CNT composite prepared by the sonication method. *Macromolecules* **42**, 8870 (2009).
21. D. Shah, P. Maiti, E. Gunn, D.F. Schmidt, D.D. Jiang, C.A. Butt, and E.P. Giannelis: Dramatic enhancements in toughness of polyvinylidene fluoride nanocomposite via nanoclay-directed crystal structure and morphology. *Adv. Mater.* **16**(14), 1173 (2004).
22. H-G. Wang, B. Mu, J-F. Ren, L-Q. Jian, J-Y. Zhang, and S-R. Yang: Mechanical and tribological behaviors of PA66/PVDF blends filled with calcium sulfate whiskers. *Polym. Compos.* **30**(9), 1326 (2009).
23. A. Fissel, B. Schroter, and W. Richter: Low-temperature growth of SiC thin- films on Si and 6H-SiC by solid-source molecular-beam epitaxy. *Appl. Phys. Lett.* **66**, 3182 (1995).
24. V.D. Krstic: Production of fine, high- purity beta silicon-carbide powders. *J. Am. Ceram. Soc.* **75**, 170 (1992).
25. V.K. Tiwari, P.K. Kulriya, D.K. Avasthi, and P. Maiti: Radiation-resistant behavior of poly(vinylidene fluoride)/layered silicate nanocomposites. *Appl. Mater. Interfaces* **1**(2), 311 (2009).
26. V.K. Tiwari, P.K. Kulriya, D.K. Avasthi, and P. Maiti: Poly (vinylidene fluoride-co-hexafluoro propylene)/layered silicate nanocomposites: The effect of swift heavy ion. *J. Phys. Chem. B* **113**, 11632 (2009).
27. S. Manna, S.K. Batabyal, and A.K. Nandi: Preparation and characterization of silver-poly(vinylidene fluoride) nanocomposites: Formation of piezoelectric polymorph of poly(vinylidene fluoride). *J. Phys. Chem. B* **110**, 12318 (2006).
28. Y. Miyamoto, H. Miyaji, and K. Asai: Anisotropy dielectric relaxation crystal form poly(vinylidene fluoride). *J. Polym. Sci., Part B: Polym. Phys.* **18**, 597 (1980).
29. A. Bello, E. Laredo, and M. Grimau: Distribution of relaxation times from dielectric spectroscopy using Monte Carlo simulated annealing: Application to alpha-PVDF. *Phys. Rev. B* **60**, 12764 (1999).
30. C.V. Chanmal and J.P. Jog: Dielectric relaxations in PVDF/BaTiO (3) nanocomposites. *Express Polym. Lett.* **2**, 294 (2008).
31. J. Mijovic, H. Lee, J. Kenny, and J. Mays: Dynamics in polymer silicate nanocomposites as studied by dielectric relaxation spectroscopy and dynamic mechanical spectroscopy. *Macromolecules* **39**, 2172 (2006).

https://doi.org/10.1557/jmr.2012.117 Published online by Cambridge University Press